14

Enhanced Dielectric and Ferroelectric Properties of Donor (W^{6+}, Eu^{3+}) Substituted SBT Ferroelectric Ceramics

Indrani Coondoo[1] and Neeraj Panwar[2]
[1]*National Physical Laboratory, Dr. K. S. Krishnan Marg,New Delhi-110012,*
[2]*Department of Physics, University of Puerto Rico, San Juan, PR-00931*
[1]*India*
[2]*USA*

1. Introduction

In recent years, there has been a tremendous interest in ferroelectric materials from perspective of their potential applications in electronic devices such as non-volatile random access memories (NvRAMs), pyroelectric infrared detectors and optical switches [1-4]. On account of their read-write speed, non volatility, low operating power and radiation hardness, NvFRAMs are promising candidates for substituting silicon based electrically erasable programmable read-only memories (EEPROMs) and flash EEPROMs. The materials for memory applications are required to possess the following properties: a large remanent polarization (P_r), a low coercive field (E_c) and sufficient fatigue endurance against repetitive polarization switching etc. [5]. Among ferroelectrics, lead zirconate titanate $PbZr_{1-x}Ti_xO_3$ (PZT) has been investigated extensively and has been found to be the most promising material for NvFRAM applications. However, apart from Pb toxicity, PZT suffers from serious degrading problems such as fatigue, ageing and leakage current that hinder the usability of this material in devices [6-10]. Among them fatigue is an important reliability issue for NvRAM devices which is defined as a decrease in switchable polarization with increasing number of polarization reversals [11].

During the search for an alternate ferroelectric material for these applications, it was found that bismuth oxide layered structures (BLSFs) originally synthesized by Aurivillius [12] are the most suitable candidates due to their relatively high Curie temperature (T_c), low dielectric dissipation and anisotropic nature originating from their layered structure [13-15]. The Aurivillius family of layered bismuth-oxides encompasses many ferroelectric materials, a fact which was known since the pioneering work of Smolenskii [16] and Subbarao [17], more than forty years ago. $SrBi_2Ta_2O_9$ (SBT), which is an n=2 member of the Aurivillius family of layered compounds, proved to be a versatile material for multifarious applications. Since Araujo et. al. [18] reported the fatigue-free behavior of $SrBi_2Ta_2O_9$ (SBT), it has gained importance among Pb-free ferroelectric memory materials [19-28]. Araujo recognized the inherent advantage of BLSFs over other ferroelectric materials on account of the fact that the former have intermediate bismuth oxide layers between the ferroelectric units [29].

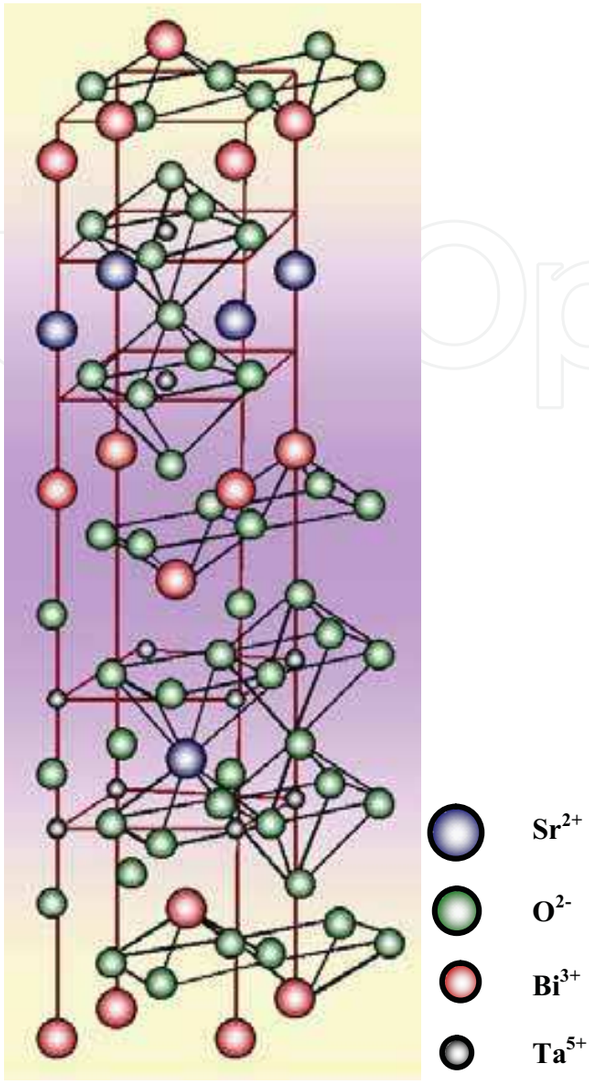

Fig. 1. The crystal structure of $SrBi_2Ta_2O_9$

Fig. 1 depicts the crystal structure of $SrBi_2Ta_2O_9$ consisting of $(Bi_2O_2)^{2+}$ layers and perovskite-type $(SrTa_2O_7)^{2-}$ units with double TaO_6 octahedral layers [30]. Besides improvement in the fatigue characteristics, a longer polarization retention time, lesser tendency to take an imprint [30,31], high dielectric constant and low switching fields have also been observed in SBT [32], which are better than those of PZT [18, 33-34]. The high fatigue endurance to repetitive switching of polarization ($\approx 10^{12}$ switching cycles) is believed to originate from the anisotropic nature of SBT. It has been argued that the $(Bi_2O_2)^{2+}$ layers control the electronic response [35-36] and perform the primary function in preventing degradation of remanent charge [35,37]. The ferroelectricity arises mainly in the perovskite blocks [15, 35, 38-40]. The dielectric constant peak corresponding to a ferro-paraelectric transition has been reported in the range of 300–320 ˚C [35, 38].Though SBT shows improved ferroelectric properties [41-42], its piezoelectric properties have not been investigated in detail. Kholkin et. al. [43] reported on the electromechanical properties of SBT but the maximum piezoelectric coefficient that was measured was quite small.

In this chapter effect of tungsten and europium substitution on dielectric, conductivity, piezoelectric and ferroelectric properties of SBT ceramics have been carried out and the results are presented.

2. Experimental techniques

The polycrystalline $SrBi_2Ta_2O_9$ (SBT) ferroelectric ceramics doped with W (tungsten) and Eu (europium) having the following compositions were prepared by the solid state reaction technique:

$$SrBi_2(Ta_{1-x}W_x)_2O_9;\ x = 0.0,\ 0.025,\ 0.050,\ 0.075,\ 0.10,\ 0.20$$

$$Sr_{1-x}Eu_xBi_2Ta_2O_9;\quad x = 0.0,\ 0.025,\ 0.050,\ 0.10,\ 0.20$$

The starting chemicals used were strontium carbonate ($SrCO_3$), bismuth oxide (Bi_2O_3), tantalum oxide (Ta_2O_5), tungsten oxide (WO_3) and europium oxide (Eu_2O_3). The chemicals were weighed in stoichiometric proportions as mentioned above. The weighed powders were mixed and thoroughly ground and passed through sieve of appropriate mesh size. The ground powder was calcined at 900 ˚C in air for two hours. Thereafter, the calcined powder was pressed into disk shaped pellets. The pellets were sintered in air at 1200 ˚C. The sintered pellets were polished to a thickness of nearly 1mm. High temperature conductive silver paste was used for electroding the parallel surfaces. After applying the silver paste, the pellets were cured at 550˚C for half an hour before electrical characterization. X-ray diffractograms of all the samples were recorded for the structural analysis using Bruker X-ray diffractometer with CuK_α radiation of wavelength 1.54439 Å in the range from $10^\circ \leq 2\theta \leq 70^\circ$ at a scanning rate of 0.05˚ / second. The SEM micrographs of the fractured surfaces of the samples were obtained using the Cambridge Stereo Scan 360 scanning electron microscope. A Solartron 1260 Gain-phase impedance analyzer was used for measuring the dielectric constant and dielectric loss in the present work. The d.c conductivity was measured using Keithley's 6517A electrometer. Hysteresis measurements were done at room temperature using an automatic PE loop tracer based on Sawyer-Tower circuit at switching frequency of 50 Hz. The piezoelectric coefecient, d_{33} was measured using a Berlincourt d_{33} meter.

3. Results and discussion

3.1 XRD analysis

The observed XRD patterns of the studied samples having different concentrations of tungsten and europium are shown in Fig. 2(a) and (b), respectively. The XRD patterns of the $SrBi_2(Ta_{1-x}W_x)_2O_9$ samples show the characteristic peaks of SBT. The peaks have been indexed with the help of a computer program – POWDIN [44] using the observed interplanar spacing d. It is observed that the single phase layered perovskite structure is maintained in the range $0.0 \leq x \leq 0.05$. An unidentified peak of very low intensity is observed in the composition with $x > 0.05$. In all the diffraction patterns, peaks shift slightly towards higher diffraction angle with increasing W concentration implying a decrease in lattice parameters. This can be understood from the fact that the ionic radius of W^{6+} (0.60Å) is smaller in comparison to Ta^{5+} (0.64Å). On the other hand no extra peaks are observed in

the XRD patterns of $Sr_{1-x}Eu_xBi_2Ta_2O_9$ samples. It can therefore be concluded that the single phase layered perovskite structure is maintained in all the SEBT samples. The calculated lattice parameters for both the series are tabulated (Table 1).

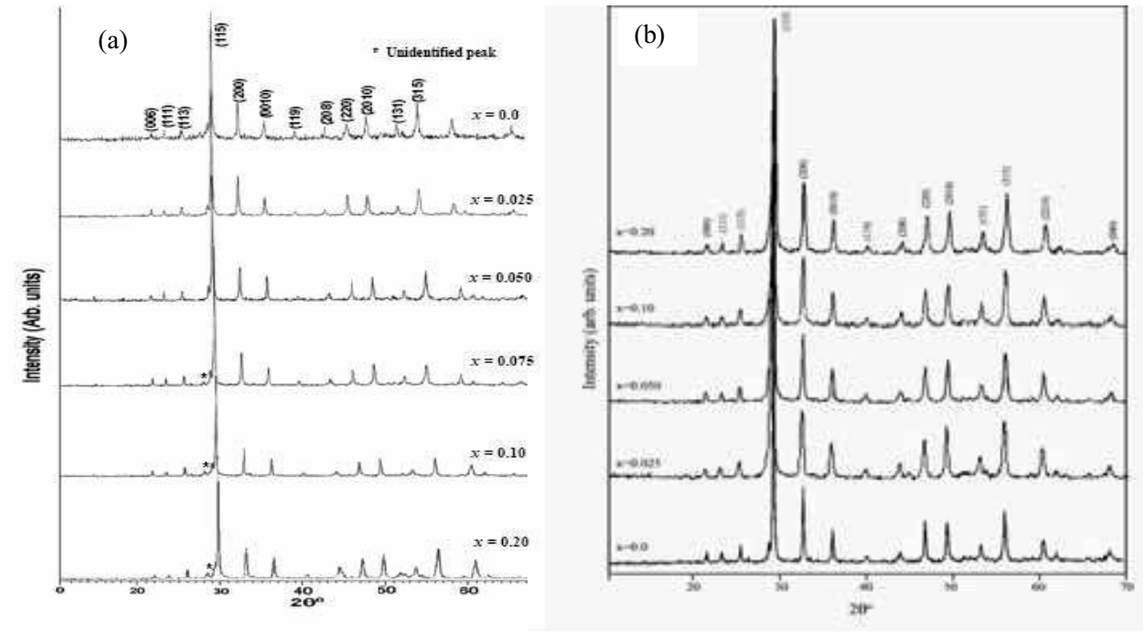

Fig. 2. XRD patterns of the (a) $SrBi_2(Ta_{1-x}W_x)_2O_9$ and (b) $Sr_{1-x}Eu_xBi_2Ta_2O_9$ samples

W Conc	*a* (Å)	*b* (Å)	*c* (Å)	Volume (Å³)	Eu Conc.	*a* (Å)	*b* (Å)	*c* (Å)	Volume (Å)³
0	5.5212	5.5139	24.9223	758.7182	**0**	5.5212	5.5139	25.0122	761.4550
0.025	5.5314	5.5202	25.1079	766.6555	**0.025**	5.5262	5.5187	25.0282	763.2960
0.05	5.5270	5.5199	25.0585	764.4969	**0.05**	5.5256	5.5158	24.9765	761.2364
0.075	5.5251	5.5045	25.0567	762.0472	**0.1**	5.5209	5.5101	24.9555	759.1641
0.1	5.5242	5.5060	25.085	762.9915	**0.2**	5.5167	5.5042	24.9349	757.1487
0.2	5.5233	5.4939	25.0861	761.2241					

Table 1. Lattice parameters and unit cell volume for $SrBi_2(Ta_{1-x}W_x)_2O_9$ and $Sr_{1-x}Eu_xBi_2Ta_2O_9$ samples

3.2 Morphological studies

Figs. 3 and 4 show the surface morphology of the SBTW and SEBT samples respectively. A systematic study of the micrographs reveals porous and loosely packed grains for the pure sample. From the figures one can notice an increase in the average grain size, homogeneity and relatively packed microstructure with W and Eu substitution. Randomly oriented and anisotropic plate-like grains are observed in all the W substituted samples. The average

grain size in the SEBT sample with x = 0.025 is ~ 5-6 μm while that in the sample with x = 0.20 the size increases to ~ 7-8 μm.

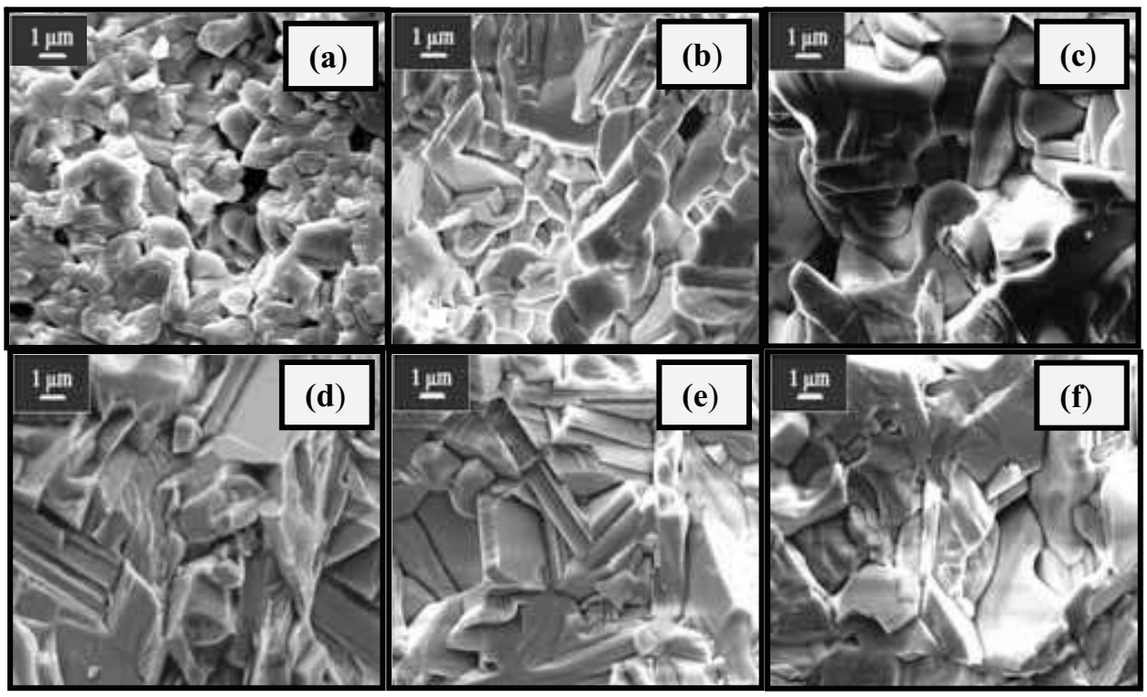

Fig. 3. SEM images with (a) x = 0.0, (b) x = 0.025, (c) x = 0.05, (d) x = 0.075, (e) x = 0.10 and (f) x = 0.20 of $SrBi_2(Ta_{1-x}W_x)_2O_9$ samples

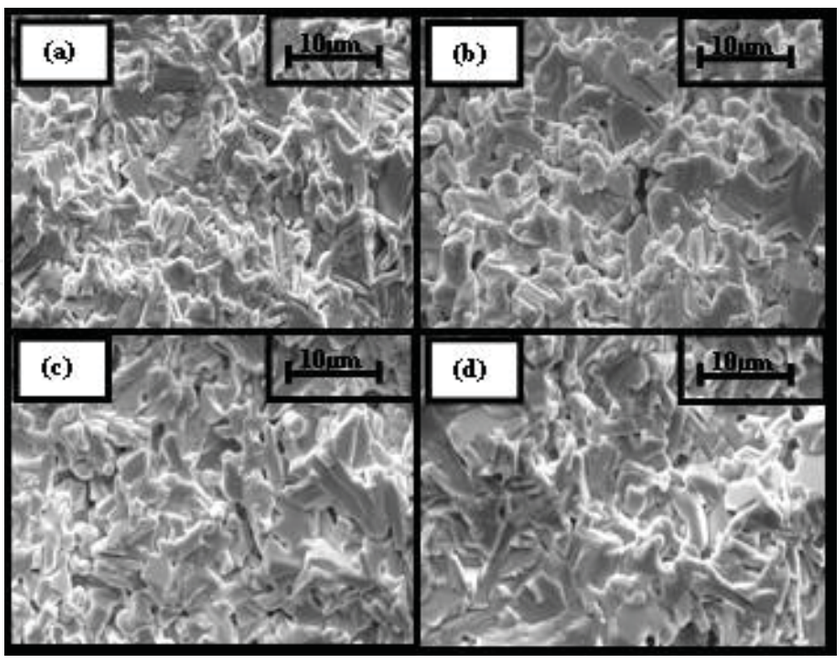

Fig. 4. SEM images with (a) x = 0.0, (b) x = 0.025, (c) x = 0.05, (d) x = 0.10 of $Sr_{1-x}Eu_xBi_2Ta_2O_9$ samples

3.3 Dielectric studies

It is well known that the dielectric permittivity and loss of ferroelectric materials in most cases depend upon the composition, grain size, secondary phases, *etc* [45]. Since bismuth layered perovskites are anisotropic in nature, its dielectric behavior is often influenced by the crystal structure [45]. All ferroelectric materials are characterized by a transition temperature known as Curie temperature (T_c) at which the dielectric constant is maximum. At temperatures $T>T_c$, the crystal does not exhibit ferroelectricity while for $T<T_c$ it is ferroelectric [46].

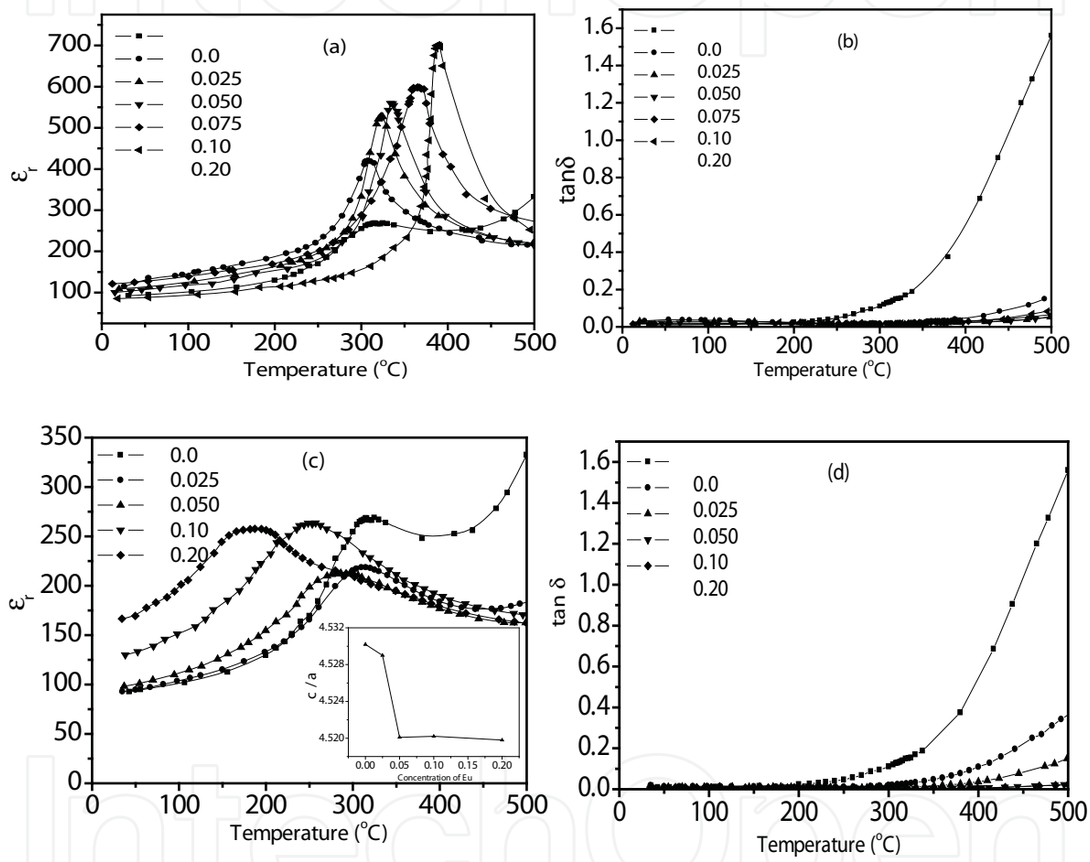

Fig. 5. (a) Temperature dependence of dielectric permittivity and (b) loss tangent for SBTW samples. (c) Temperature dependence of dielectric permittivity and (d) loss tangent for SEBT samples. The inset in (c) shows variation of tetragonal strain (c/a) with Eu concentration

The phase transition temperature of a sample is deduced from its dielectric permittivity (ε_r) versus temperature curve. Fig. 5(a) shows the temperature dependence of ε_r at selected frequencies of 100 kHz in SBTW samples. All the doped samples exhibit sharp transition at their respective Curie temperatures (T_c). A shift in T_c to higher temperatures and a corresponding increase in the peak dielectric constant values with increasing concentration of tungsten are observed.

The observed variation in T_c & peak-ε_r with concentration is explained in the ensuing paragraph. Generally in isotropic perovskite ferroelectrics, doping at *B*-site (located inside an oxygen octahedron) with smaller ions results in the shift of the Curie point to a higher temperature, leading to a larger polarization due to the enlarged "rattling space" available for smaller *B*-site ions [37]. However, in the anisotropic layered-perovskites, the crystal structure may not change as freely as that in the isotropic perovskites with doping due to the structural constraint imposed by the $(Bi_2O_2)^{2+}$ interlayer [47-48]. On comparing the variation of in-plane lattice parameters *a* and *b* (Table 1) with tungsten concentration, we observe that with increasing tungsten concentration a decrease in the lattice parameters *a* and *b* is observed. It is this enhancement of ferroelectric structural distortion along with the introduction of cation vacancies at the *A*-site that lead to an eventual increase in T_c value [21, 25, 47, 49-50]. In Fig. 5 (a) it is observed that peak-ε_r increases with increasing tungsten concentration. The high T_c which is indicative of enhanced polarizability [21, 36, 51-52], explains the increase in peak ε_r. Moreover, since the valency of the substitutional cation (W^{6+}) is higher than the Ta^{5+}, the substitution creates cationic vacancies at Sr-site ($V_{Sr}^{''}$) to maintain electrical neutrality of the lattice structure [22, 47, 53]. In the tungsten doped samples, because of the constraint of maintaining overall charge neutrality of the structure, substitution of W^{6+} ions for Ta^{5+} in the structure result in the formation of cation vacancies at *A*-sites. For substitution of two W^{6+} ions, one *A*-site (Sr site) remains vacant. The process can be represented as:

$$Null = W_{Ta}^{\bullet} + \frac{1}{2}V_{Sr}^{''} \tag{1}$$

where $W_{Ta}^{\bullet}$ represents tungsten replacing tantalum site and $V_{Sr}^{''}$ denotes the Sr-vacant site. It has been reported that cation vacancies make the domain motion easier and increase the dielectric permittivity [53-54] and thus an increase in ε_r with increasing W content is observed. There is also a possibility that the microstructural development due to compositional deviation from the stoichiometry affect the dielectric properties. It is expected that the domain walls are quite free in their movement in larger grains than smaller sized grains, since grain boundaries contribute additional pinning points for the moving walls [55-56]. Increase in the grain size makes the domain wall motion easier which results in an increase in the dielectric permittivity [41]. Since the grain size increases with sintering W concentration (Fig. 3), an increase in peak - ε_r is observed.

Fig. 5 (b) shows the tangent loss (tanδ) as a function of temperature in W-doped samples measured at 100 kHz. It is observed that tungsten doping in SBT reduces dielectric loss significantly. The dissipation in ferroelectric materials occurs due to various causes such as domain wall relaxation, space charge accumulation at grain boundaries, dipolar losses, dc conductivity, *etc.* [45]. The presence of oxygen vacancies $V_o^{\bullet\bullet}$, which act as space charge and contribute to the electrical polarization can be related to the dielectric loss [50, 57-58]. The substitution of W^{6+} for Ta^{5+} in SBT results in the formation of cation vacancies which effectively reduces the concentration of oxygen vacancies which in turn significantly reduce the dielectric loss. Reduction in loss have been reported in other donor doped BLSFs also [25, 49].

Fig. 5(c) shows the temperature dependence of dielectric permittivity at 100 kHz for SEBT samples. The substitution of Eu in SBT lowers and broadens the ferro-paraelectric phase transition temperature. The broadened peaks, as observed in Fig. 5c, indicate that transition in all the samples is of diffuse type, an important characteristic of a disordered perovskite structure [59]. The broad peak implies that the ferroelectric - paraelectric phase transition does not occur at discrete temperature but over a temperature range [11]. The broadening or diffuseness of peak occurs mainly due to two mechanisms. One is due to the substitution disordering in the arrangement of cations at one or more crystallographic sites in the lattice structure leading to heterogenous domains [60]. Another possible explanation of broadened peak is due to the defect induced relaxation at high temperature [60-61].

Comprehensive structural analysis of SBT with the aid of neutron diffraction and Raman scattering have shown disorder in the distribution of the Sr ions and Bi ions [62-63]. Recent independent studies by Ismunandar *et. al*. [64] and Blake *et. al*. [62] have reported that there is a significant degree of Sr/Bi cation disorder in the $SrBi_2Nb_2O_9$ compounds. Thus, it is possible that cation disorder between Sr and Bi sites also occurs in the tantalum analogues [51, 66]. Macquart *et. al*. [67], provided conclusive evidence of cation disorder in $ABi_2Ta_2O_9$, where *A* = Ca, Ba, Sr. As already mentioned pristine $SrBi_2Ta_2O_9$ is not perfectly stoichiometric and contains a certain amount of inherent defects (*e.g.* oxygen vacancies) resulting from the volatilization of Bi_2O_3 at high temperatures. When Bi_2O_3 is lost, bismuth and oxygen vacancy complexes are formed in the $(Bi_2O_2)^{2+}$ layers [58, 68]. Hence, such disorder in the arrangements of cations at A-sites (in perovskite- like unit) and Bi sites (in Bi_2O_2 layers) is likely to be present. It is because of the cation disordering, that ions at *A* and *B* site are not homogenously distributed on a microscopic scale. Such compositional fluctuations lead to a microscopic heterogeneity in the structure that consists of microdomains having slightly different chemical compositions [69-70]. These microdomains with different chemical compositions will have different ferro-paraelectric transition temperatures. This distribution of T_c induces a gradual ferroelectric transition leading to broadening of the peak [48, 69-71]. In the context of above discussions, it is highly probable that some Eu^{3+} ions, in addition to occupying Sr^{2+} sites, also occupy the available bismuth vacant sites in the Bi_2O_2 layer. In other words, there is a possibility of inhomogenous distribution of Eu ions in perovskite blocks and $(Bi_2O_2)^{2+}$ layers. This can be expressed as:

$$Eu^{\bullet\bullet\bullet} + V_{Bi}^{'''} = Eu_{Bi} = Null \tag{2}$$

The above expression denotes the occupancy of Eu ion ($Eu^{\bullet\bullet\bullet}$) at the vacant Bi site ($V_{Bi}^{'''}$); since Eu has +3 charge and Bi vacancy has effective -3 charge, they neutralize each other. Thus, it is reasonable to believe that the observed broadening of dielectric peak in Eu substituted SBT, is due to the oxygen vacancy-induced-dielectric relaxation [60-61, 72] and not a result of diffused phase transition as in a relaxor ferroelectric since we did not observe frequency dependence of T_c for SEBT.

The fall in Curie temperature for SEBT samples can be understood in terms of the observed tetragonal strain variation (inset of Fig. 5c). Tetragonal strain is the internal strain in the lattice, which is reported to affect the phase transition temperature [52, 73-75]. Smaller value of strain indicates that lesser amount of thermal energy is required for the phase transition and therefore a decrease in T_c is expected with a decrease in the strain, as indeed observed. Dielectric measurements reported in other works have also shown that the introduction of

rare-earth ions at the *A* site in various perovskites and layered oxides, decreases ferroelectric phase transition temperature [76-78]. Curie temperature of Pr substituted SBT has been reported to be lower than that of SBT [77]. Dielectric measurements of La-substituted $PbTiO_3$ have revealed a decrease in T_c [79]. It is also reported that with increasing La content in SBT, the dielectric peak broadens and the Curie temperature decreases [42]. Nd has been substituted at *A*-site in $Bi_4Ti_3O_{12}$ (BIT) which resulted in decrease of T_c [80]. Vaibhav *et. al.* [74] have reported that La substitution in $SrBi_2Nb_2O_9$ result in a decrease of T_c with broadened peak. Watanabe *et. al.* [80] reported that lanthanoids like Nd and Pr substitutions effectively decrease T_c in BIT. Therefore, since Eu is a rare-earth ion, it is plausible that with increase in the content of europium, T_c decreases with broadened peak around the transition temperature. In addition, it is also known that the incorporation of cations into $(Bi_2O_2)^{2+}$ layers reduces their electrostatic influence on the perovskite blocks, which might further contribute to the lowering of phase-transition [48, 81]. As discussed above, some of the Eu^{3+} also occupies the available vacant bismuth sites in the bismuth-oxide layer and therefore a decrease in the phase transition temperature is observed. Possibly all the above discussed mechanisms contribute partially to the observed dielectric behavior of the studied compositions.

Fig. 5(d) shows the temperature dependence of tangent loss at 100 kHz for SEBT samples. It is observed that europium doping reduces the dielectric loss. The loss of Bi_2O_3 during sintering process results in the formation of $V_o^{\bullet\bullet}$ in SBT [82]. The additional charge in case of donor substituted compounds is compensated through the formation of cation vacancies to maintain the overall charge neutrality of the unit structure. Similar observations have been made in rare-earth (La^{3+},Nd^{3+}, Ce^{3+}, Sm^{3+}) substituted SBT [39, 42,76-77]. Based on the above reports and the present observations it is reasonable to believe that the substitution of trivalent Eu ions for divalent Sr ions results in the formation of cation vacancies at the *A* sites. For maintaining the charge neutrality of the unit structure, on the substitution of two Eu^{3+} ions, one *A*-site (Sr site) remains vacant. The corresponding formation of vacancy can be represented as:

$$Null = Eu_{Sr}^{\bullet} + \frac{1}{2}V_{sr}^{''} \tag{3}$$

where $V_{Sr}^{''}$ denotes the strontium vacant site; $Eu_{Sr}^{\bullet}$ denotes Eu occupying the Sr site. Thus, it can be inferred that in Eu added SBT, the charge difference between Sr^{2+} and Eu^{3+} is compensated by the formation of Sr vacancies $V_{Sr}^{''}$. Since $V_{Sr}^{''}$ are effectively negatively charged and $V_o^{\bullet\bullet}$ are effectively positively charged, these $V_{Sr}^{''}$ reduce the number of $V_o^{\bullet\bullet}$ and thereby reduce the dielectric loss.

3.4 dc conductivity

The electrical conductivity of ceramic materials encompasses a wide range of values. The conductivity is usually strongly dependent upon temperature and composition [83]. In insulators charge carriers are regarded as defects in the perfect crystalline order, and the consideration of charge transport leads necessarily to consideration of point defects and their migration [84].

Pure SBT has inherent oxygen vacancies that are effectively doubly positively charged, and thus behave as acceptor-excess material [85]. The apparent net excess of acceptor content in

pure SBT can be suppressed by addition of donors that reduces the oxygen vacancy concentration [85]. It has been reported that conductivity in $Bi_4Ti_3O_{12}$ (BIT) can be significantly decreased with the addition of donors, such as Nb, Sb and Ta [86-88]. Makovec et. al. [39] reported that the minimum conductivity in air-sintered $BaBi_4Ti_4O_{15}$ ceramics was obtained by the substitution of ~ 5 mol% of the Ti^{4+} ions with Nb^{5+} donors, and this resulted in a conductivity decrease of two orders of magnitude. Therefore, it is reasonable to believe that the conductivity in SBT can be suppressed by donor addition.

Fig. 6(a) and (b) shows the temperature dependence of dc conductivity (σ_{dc}) for SBTW and SEBT samples, respectively. The curves show that the conductivity increases with temperature. This suggests the presence of negative temperature coefficient of resistance (NTCR), which is a characteristic of insulators [84]. It is observed that d.c. conductivity reduces with both W and Eu substitution in SBT. Two predominant conduction mechanisms indicated by slope changes in two different temperature regions are observed. Such change in the slope in the vicinity of the Curie temperature is attributed to the differences in the activation energy values in the ferroelectric and paraelectric regions. The temperature region of ~300 ˚C to ~700 ˚C in these ceramics corresponds to the intrinsic ionic conduction range [86, 89]. In Table 2 the activation energies in the intrinsic conduction region, calculated using the Arrhenius equation for all the studied samples are given. The E_a value of the W and Eu substituted samples is much higher than that of the pure sample.

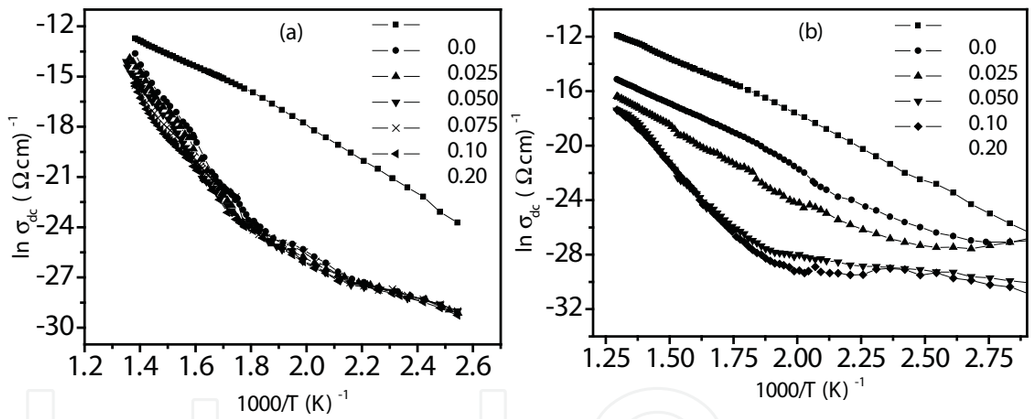

Fig. 6. Variation of dc conductivity with temperature for (a) SBTW and (b) SEBT samples

W in SBT	E_a (eV)	**Eu in SBT**	E_a (eV)
0.0	0.76	**0.0**	0.69
0.025	1.92	**0.025**	0.77
0.05	1.96	**0.05**	0.96
0.075	1.98	**0.1**	1.59
0.10	1.86	**0.2**	1.73
0.20	1.74		

Table 2. Activation energy (E_a) values obtained in high temperature region for $SrBi_2(Ta_{1-x}W_x)_2O_9$ and $Sr_{1-x}Eu_xBi_2Ta_2O_9$ samples

It is known that the major disadvantage of the layer-structured perovskite materials for certain applications is their relatively high conductivity [90]. The high conductivity observed in layer-structured perovskite materials is related to the presence of oxygen vacancies which are effectively positively charged defects or acceptor impurities. The concentration of these defects and, consequently, the material's conductivity, thus, increases by acceptor doping and decreases by donor doping [83-84, 89, 91-93]. Similarly in our case we observed a decrease in conductivity with donor (W and Eu) substitution in SBT. The constraint of maintaining the overall charge neutrality of the structure generates cation vacancies at Sr sites. These cation vacancies thus formed (represented by Eqs. 1 and 3), effectively reduces the concentration of oxygen vacancies. The effect of both W and Eu substitution on the concentration of oxygen vacancies is verified from the dc conductivity measurements since a decrease in dc conductivity is observed in both cases.

It is observed in Table 2 that the E_a values increases with increasing Eu content. As the concentration of Eu increases, more and more oxygen vacancies are compensated for and thereby the energy needed for the charge carriers to migrate (by hopping) also increases, leading to higher activation energy. As a result, the conductivity decreases because there are fewer oxygen vacancies available with sufficient energy to move around and the energy barrier between the scarcer vacancies increases [86]. Whereas in W-substituted samples E_a is observed to increase with W concentration up to $x = 0.05$; however, beyond that it decreases (Table 2). The decrease in the activation energy for samples with $x > 0.05$ suggests an increase in the concentration of mobile charge carriers [94]. This observation can be ascribed to the existence of multiple valence states of tungsten. Since tungsten is a transition element, the valence state of W ions in a solid solution most likely varies from W^{6+} to W^{4+} depending on the surrounding chemical environment [95-96]. When W^{4+} are substituted for Ta^{5+} sites, oxygen vacancies would be created, i.e. one oxygen vacancy would be created for every two tetravalent W ions entering the crystal structure increasing the concentration of mobile charge carriers and consequently a decrease in the E_a beyond $x > 0.05$.

The observed variation in conductivity with tungsten and europium content in SBT is consistent with dielectric loss, which also reduces with increasing tungsten concentration and has been explained in light of contribution from oxygen vacancies.

3.5 Ferroelectric properties

The P-E loops measured at 50 Hz and room temperature for SBTW and SEBT samples are shown in Fig. 7 (a) and (b), respectively. It is observed that W-substitution results in the formation of well-defined hysteresis loops. The optimum tungsten content for maximum $2P_r$ (~ 25 $\mu C/cm^2$) is observed to be $x = 0.075$.

It is known that ferroelectric properties are affected by compositional modification, microstructure and lattice defects like oxygen vacancies within the structure of the materials [15-26, 97]. In hard ferroelectrics, with lower-valent substituents the associated oxide vacancies are likely to assemble in the vicinity of domain walls [43, 98-99]. These domains are locked by the defects and their polarization switching is difficult, leading to a decrease in P_r and an increase in E_c. Moreover, theoretical calculations [100] have also shown that the increase in space charge density brings about a decrease in P_r. On the other hand, in soft ferroelectrics, with higher-valent substituents, the defects are cation vacancies whose

mobility is extremely low below T_c. Thus, the interaction between cation vacancies and domain walls is much weaker than that in hard ferroelectrics [38, 43] leading to an increase in P_r values. Watanabe et. al. [101] reported a remarkable improvement in ferroelectric properties in the $Bi_4Ti_3O_{12}$ ceramic by adding higher valent cation, V^{5+} at the Ti^{4+} site. Recently, significantly large P_r value has been reported for W-substituted BIT sintered sample [102]. It has also been reported that cation vacancies generated by donor doping make domain motion easier and enhance the ferroelectric properties [103]. Also it is known that domain walls are relatively free in large grains and are inhibited in their movement as the grain size decreases [45]. In the larger grains, domain motion is easier which results in larger P_r [104-105].

Based on the obtained results and above discussion, it can be understood that in pure SBT, the oxygen vacancies assemble at sites like domain boundaries leading to a strong domain pinning. Hence well-saturated P-E loops for pure SBT are not obtained. Whereas, in the W-substituted samples, the associated cation vacancy formation suppresses the concentration of oxygen vacancies. A reduction in the number of oxygen vacancies reduces the pinning effect on the domain walls, leading to enhanced remnant polarization and lower coercive field. Another possible reason could be attributed to the increase in grain size of SBTW, as observed in SEM micrographs (Fig. 3). In the present study, the grain size is observed to increase with increasing W concentration; however, the remanent polarization does not monotonously increase with increasing W concentration (Fig. 7a). It is observed that beyond $x > 0.075$ P_r values decreases. Therefore, besides the effect of grain size and reduction in oxygen vacancies, other factors also influence variation in remnant polarization.

The decrease in the value of $2P_r$ for $x > 0.075$, seems possibly due to the presence of secondary phases (observed in XRD diffractograms) which hampers the switching process of polarization [106-110]. Also this could be explained on the basis of the inference drawn w.r.t. dc conductivity study in SBTW. We concluded that beyond $x > 0.05$, the number of charge carriers increases in the form of oxygen vacancies. This increase in oxygen vacancies beyond $x > 0.05$ leads to pinning of domain walls and thus a reduction in the P_r values is observed [111].

Fig. 7 (b) shows the P-E loops of the SEBT samples. It is observed that the remanent polarization increase with increase in europium content. The maximum $2P_r$ ~14 $\mu C/cm^2$ is observed in the sample with $x = 0.20$. A lot of studies on the influence of rare-earth ion substitution in simple perovskite ferroelectrics have shown improved ferroelectric properties [88, 112-115]. The substitution of smaller lanthanoid ions like Samarium (Sm^{3+}), Neodium (Nd^{3+}) and lanthanum (La^{3+}) etc. into BIT is reported to enhance remnant polarization [25, 116-118]. $SrBi_4Ti_4O_{15}$, which has a crystalline structure similar to BIT, is another typical BLSF (m = 4) that shows enhanced ferroelectric properties as a result of La doping [119]. Noguchi et. al. [76] have reported that La, Nd, and Sm substitution in SBT show a large P_r compared to pure SBT. These results suggest that the smaller rare earth ion substitution enhances ferroelectric properties. Also, the substitution of Sr^{2+} by Eu^{3+} in the SBT lattice, results in the formation of vacancies at the A site (V''_{Sr}) that suppresses the concentration of oxygen vacancies leading to the observed enhancement of remnant polarization (Fig. 7b).

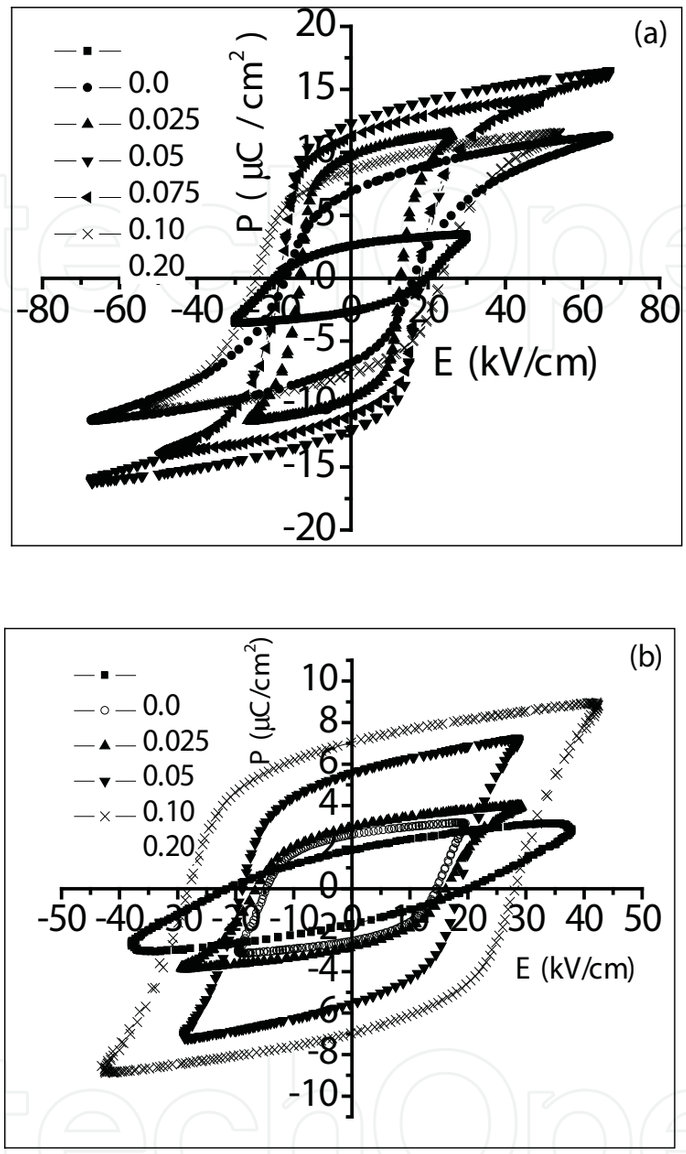

Fig. 7. P-E hysteresis loops for (a) SBTW and (b) SEBT samples

3.6 Piezoelectric studies

Piezoelectric ceramics are widely used for electromechanical transducers and hydrostatic sensing applications. Among the available materials, lead zirconate titanate (PZT) exhibits a large piezoelectric coefficient, d_{33} (400–600 pC/N) [120]. In recent years, lead-free materials such as bismuth-layered structured ferroelectrics (BLSFs) have been attracting attention for piezoelectric device applications, and are found suitable for fine tolerance resonators with excellent frequency stability [121]. Ando *et. al.* [122] have reported the effects of

compositional modifications in strontium bismuth niobate (SBN)-based BLSF materials in improving the piezoelectric properties. Kholkin *et. al.* [43] has reported on the electromechanical properties of SBT but the maximum polarization and piezoelectric coefficient that were measured were quite small. Since BLSFs generally have high Curie temperature and high coercive field at room temperature, it is necessary to perform poling at high temperature [123]. However, relatively high conductivity often prevents the application of high electrical field during the high-temperature poling treatment [123-124]. The conductivity, therefore, should be reduced in BLSFs to increase the poling efficiency.

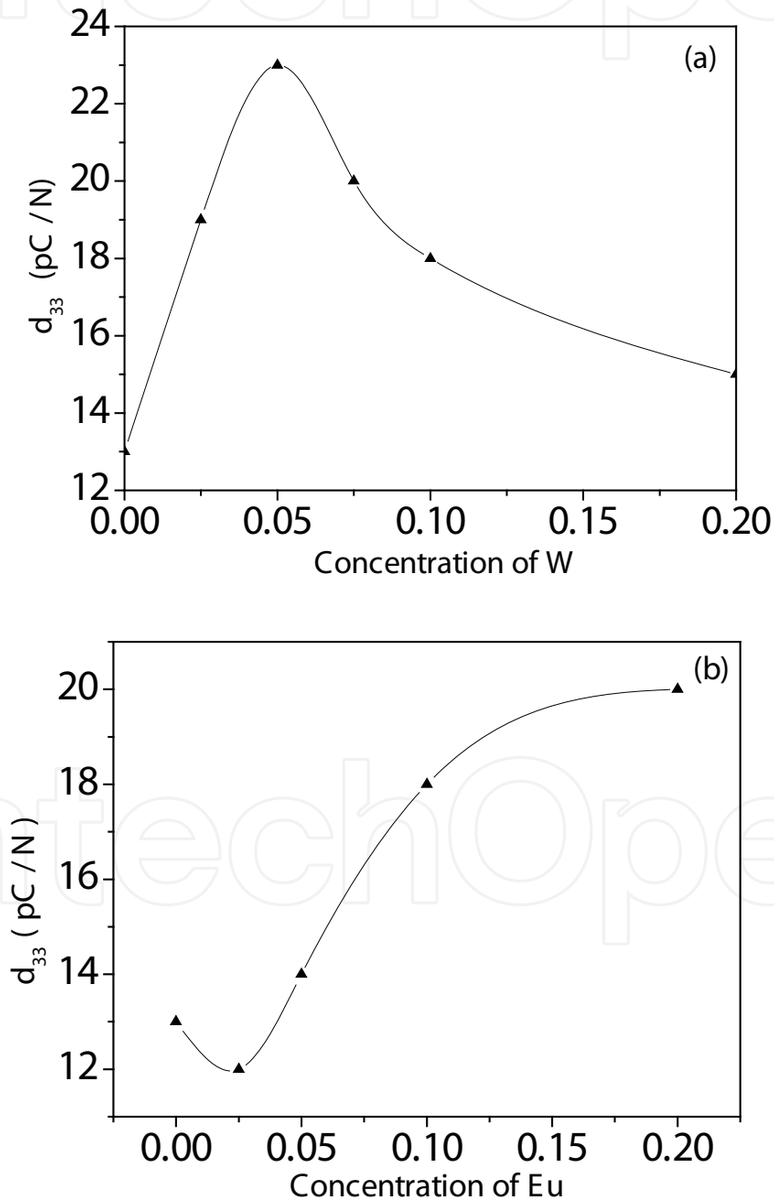

Fig. 8. Variation of d_{33} in (a) SBTW and (b) SEBT samples

Fig. 8(a) and (b) shows the variation of piezoelectric charge coefficient d_{33} with x in SBTW and SEBT samples, respectively. The d_{33} increases with *x* up to *x* = 0.05, however, d_{33} did not improve significantly. A decrease in d_{33} values is observed for the samples with x > 0.05.
The piezoelectric coefficient, d_{33}, increases from 13 pC/N in the sample with x = 0.0 to 23 pC/N in the sample with x = 0.05 in SBTW. Whereas in SEBT samples, the coefficient is observed to increase from 13 (x =0.0) to 20 pC/N (x = 0.20). The above observation can be explained on the basis of conductivity behavior observed in W- and Eu-substituted SBT samples. As observed, electrical conductivity reduces with both donor substituents (Fig. 6a and b) in SBT. This decrease in conductivity upon donor substitution improves the poling efficiency and thus higher d_{33} values are obtained. It has also been reported that the incorporation of higher valent ions accompanied with cation vacancies at the *A* site in BLSFs, improves not only the ferroelectric property but also the piezoelectric one [49, 125]. The piezoelectric constants have also been found to increase with increase in grain size [49]. The report that the vacancies at *A* sites improve the piezoelectric properties due to increased wall mobility, supports the present observation in both cases. Moreover, since the grain size increases with both W and Eu content (Figs. 3 and 4), it is reasonable to believe that the increase in grain size will also contribute to the increase in d_{33} values. The decrease in the value of d_{33} for samples with x > 0.05 in SBTW samples is possibly due to the presence of secondary phases [1, 126-127] in the samples discussed earlier with respect to XRD observations (Fig. 2a).

4. Conclusions

The addition of tungsten in SBT is observed to be effective in improving dielectric, electrical, ferroelectric and piezoelectric properties. The X-ray diffractograms show the formation of the single phase layered structure up to W concentration x ≤ 0.05, beyond which an unidentified peak is observed though its intensity is very small. Scanning Electron Microscopy (SEM) photographs reveal that W addition in SBT is effective in improving the microstructure, as, well developed dense microstructure with large grains are seen. The average grain size increases with increase in W content. The substitution of the smaller W^{6+} ions for Ta^{5+} ions in SBT is found to be effective in improving the dielectric properties. Dielectric constant (ε_r) and the Curie temperature (T_c) increases with increasing W content. The dielectric loss reduces significantly with increase in doping level. The maximum T_c of ~ 390 ˚C is observed in the sample with x = 0.20 as compared to ~ 320 ˚C for the pure sample. The peak - ε_r increases from ~ 270 in the sample with x = 0.0 to ~ 700 for the composition with x = 0.20. The temperature dependence of the electrical conductivity shows that tungsten doping results in the decrease of conductivity by as much as 2-3 orders of magnitude compared to pure SBT. All the tungsten-doped ceramics have higher $2P_r$ than that in the pure sample. The maximum $2P_r$ (~25 $\mu C/cm^2$) is obtained in the composition with x=0.05. The d_{33} values increase with increasing W content up to x ≤ 0.05. The value of d_{33} in the composition with x = 0.05 is ~ 23 pC/N as compared to ~ 13 pC/N in the pure sample.
For the europium-substituted samples, the single phase structure is maintained for the entire concentration range. The lattice parameters decrease with increase in europium concentration. The average grain size increases with increasing Eu concentration. It is

observed that the studied samples undergo a diffused transition near T_c. The dielectric loss and conductivity reduces with increasing Eu content. An increase in remanent polarization has been observed with increasing Eu content. The maximum $2P_r$ value of ~ 14 $\mu C/cm^2$ is observed in the sample with x = 0.20 as compared to 4 $\mu C/cm^2$ for the pure sample. A maximum d_{33} of ~ 20 pC/N is obtained in the sample with x = 0.20 as compared to 13 pC/N for the pure sample.

Thus, addition of both the donor cations, W^{6+} and Eu^{3+} in SBT, is found to be effective in improving microstructural, electrical, ferroelectric and piezoelectric properties. Addition of both the donors, result in increase in grain size which makes domain motion easier and thereby enhance the dielectric permittivity, remanent polarization and d_{33} values. Also, the associated cation vacancies that are formed to maintain the charge neutrality in the structure is known to make domain motion easier. This contributes further in enhancing the various properties mentioned above. Also, W and Eu doping in SBT results in reduced dielectric loss and conductivity. Such compositions with low conductivity and high P_r values should be excellent materials for highly stable ferroelectric memory devices.

5. References

[1] J. F. Scott and C. A. P. de Araujo, *Science*, 246, 1400 (1989).
[2] G. H. Haertling, *J. Vac. Sci. Tech.*, 9, 414 (1990).
[3] J. J. Lee, C. L. Thio and S. B. Desu, *J. Appl. Phys.*, 78, 5073 (1995).
[4] S. Dey and R. Zuleeg, *Ferroelectrics*, 108, 37 (1990).
[5] A. Kitamura, Y. Noguchi and M. Miyayama, *Mater. Lett.*, 58, 1815 (2004).
[6] H. N. Al-Shareef, A. I. Kingon, X. Chen, K. R. Bellur and O. Auciello, *J. Mater. Res.*, 9, 2986 (1994).
[7] W. L. Warren, D. Dimos, B. A. Tuttle, R. D. Nasby and G. E. Pike, *Appl. Phys. Lett.*, 65, 1018 (1994).
[8] J. F. Chang and S. B. Desu, *J. Mater. Res.*, 9, 955 (1994).
[9] K. Amanuma, T. Hase and Y. Miyasaka, *Jpn. J. Appl. Phys.*, 33, 5211 (1994).
[10] P. C. Joshi and S. B. Krupanidhi, *J. Appl. Phys.*, 72, 5827 (1992).
[11] Y. Zhu, X. Zhang, P. Gu, P. C. Joshi and S. B. Desu, *J. Phys.: Condens. Matter*, 9, 10225 (1997).
[12] B. Aurivillius, *Ark. Kemi*, 1, 463 (1949).
[13] B. Aurivillius, *Ark. Kemi*, 1, 499 (1949).
[14] R. L. Withers, J. G. Thompson, L. R. Wallenberg, J. D. FitzGerald, J. S. Anderson and B. G. Hyde, *J. Phys. C: Solid State Phys.*, 21, 6067 (1988).
[15] R. L. Withers, J. G. Thompson and A. D. Rae, *J. Solid State Chem.*, 94, 404 (1991).
[16] G. A. Smolenskii, V. A. Isupov and A. I. Agranovskaya, *Sov. Phys. Solid State*, 3, 651 (1959).
[17] E. C. Subbarao, *J. Phys. Chem. Solids*, 23, 665 (1962).
[18] C. A. P. de Araujo, J. D. Cuchiaro, L. D. Macmillan, M. C. Scott & J. F. Scott, *Nature* (London) 374, 627 (1995).
[19] M. Hirose, T. Suzuki, H. Oka, K. Itakura, Y. Miyauchi and T. Tsukada, *Jpn. J. Appl. Phys.*, 38, 5561 (1999).
[20] M. Kimura, T. Sawada, A. Ando and Y. Sakabe, *Jpn. J. Appl. Phys.*, 38, 5557 (1999).

[21] T. Takeuchi, T. Tani and Y. Saito, *Jpn. J. Appl. Phys*., 39, 5577 (2000).
[22] T. Mihara, H. Yoshimori, H. Watanabe and C. A. P. de Araujo, *Jpn. J. Appl. Phys*., 34, 5233 (1995).
[23] K. Kato, C. Zheng, J. M. Finder, S. K. Dey and Y. Torii, *J. Am. Ceram. Soc*., 81, 1869 (1998).
[24] E. Tokumitsu, G. Fujii and H. Ishiwara, *Mater. Res. Symp. Proc*., 493, 459 (1998).
[25] B. H. Park, B. S. Kang, S. D. Bu, T. W. Noh, J. Lee and W. Joe, *Nature*, 401, 682 (1999).
[26] K. Ishikawa and H. Funakubo, *Appl. Phys. Lett*., 75, 1970 (1999).
[27] A. Gruverman, A. Pignolet, K. M. Satyalakshmi, M. Alexe, N. D. Zakharov and D. Hesse, *Appl. Phys. Lett*., 76, 106 (2000).
[28] J. Lettieri, M. A. Zurbuchen, Y. Jia, D. G. Schlom, S. K. Streiffer and M.E. Hawley, *Appl. Phys. Lett*., 77, 3090 (2000).
[29] A. R. James, S. Balaji and S. B. Krupanidhi, *Mater. Sci. Engi*. B64, 149 (1999).
[30] R. Jain, V. Gupta and K. Sreenivas, *Mater. Sci. Engi.* B78, 63 (2000).
[31] J. Zhang, Z. Yin and M. S. Zhang, *Appl. Phys. Lett*., 81(25) 4778 (2002).
[32] K. Amanuma, T. Hase and Y. Miyasaka, *Appl. Phys. Lett*., 66, 2 (1995).
[33] J. F. Scott, *Phys. World*, 46, 22 (1995).
[34] O. Auciello, J. F. Scott and R. Ramesh, *Phys. Today*, 51, 22 (1998).
[35] S. K. Kim, M. Miyayama and H. Yanagida, *Mater. Res. Bull*., 31, 121(1996).
[36] M. G. Stachiotti, C. O. Rodriguez, C. A. Draxl & N. E. Christensen, *Phys. Rev*., B61, 14434 (2000).
[37] Y. Noguchi, M. Miyayama and T. Kudo, *Phys. Rev*., B63, 214102 (2001).
[38] A. D. Rae, J. G. Thompson and R. L. Withers, *Acta. Crystallogr. Sect*., B48, 418 (1992).
[39] Y. Shimakawa, Y. Kubo, Y. Nakagawa, T. Kamiyama, H. Asano and F. Izumi, *Appl. Phys. Lett*., 74, 1904 (1998).
[40] S. M. Blake, M. J. Falconer, M. McCreedy and P. Lightfoot, *J. Mater. Chem*., 7, 1609 (1997).
[41] A. Li, H. Ling, D. Wu, T. Yu, M. Wang, X. Yin, Z. Liu and N. Ming, *Appl. Surf. Sci*., 173, 307 (2001).
[42] T. Noguchi, T. Hase and Y. Miyasaka, *Jpn. J. Appl. Phys*., 35, 4900 (1996).
[43] A. L. Kholkin, K. G. Brooks and N. Setter, *Appl. Phys. Lett*., 71, 2044 (1997).
[44] Wu, E., POWD, *An interactive powder diffraction data interpretation and indexing program* Ver2.1, School of Physical Science, Flinders University of South Australia, Bedford Park S.A. JO42AU.
[45] R. R. Das, P. Bhattacharya, W. Perez & R. S. Katiyar, *Ceram. Int*., 30, 1175 (2004).
[46] M. Deri, *Ferroelectric Ceramics* (Akademiai Kiado, Budapest, 1966).
[47] Y. Wu, C. Nguyen, S. Seraji, M. J. Forbess, S. J. Limmer, T. Chou and G. Z. Cao, *J. Amer. Ceram. Soc*., 84, 2882 (2001).
[48] P. D. Martin, A. Castro, P. Millan and B. Jimenez, *J. Mater. Res*., 13, 2565 (1998).
[49] H. T. Martirena and J. C. Burfoot, *J. Phys. C: Solid State Phys*., 7, 3182 (1974).
[50] Y. Wu, C. Nguyen, S. Seraji, M. J. Forbess, S. J. Limmer, T. Chou and G. Z. Cao, *J. Amer. Ceram. Soc*., 84, 2882 (2001).
[51] Y. Shimakawa, Y. Kubo, Y. Nakagawa, T. Kamiyama, H. Asano and F. Izumi, *Phys. Rev*., B61, 6559 (2000).
[52] C. Prakash and A. S. Bhalla, *Ferroelectrics*, 262, 321 (2001).
[53] Y. Noguchi, M. Miyayama and T. Kudo, *J. Appl. Phys*., 88, 2146 (2000).

[54] K. Singh, D. K. Bopardik and D. V. Atkare, *Ferroelectrics*, 82, 55 (1988).
[55] E. C. Subbarao, *Integrat. Ferro*., 12, 33 (1996).
[56] Y. Wu, S. J. Limmer, T. P. Chou and C. Nguyen, *J. Mater. Sci. Lett*., 21, 947 (2002).
[57] I. Coondoo, A. K. Jha and S. K. Agarwal, *Ceram. Int*., 33, 41 (2007).
[58] I. Coondoo, A. K. Jha and S.K. Agarwal, *J. Eur. Ceram. Soc*., 27, 253 (2007).
[59] R. Rai, S. Sharma and R. N. P. Choudhary, *Solid State Commu*., 133, 635 (2005).
[60] R. Rai, S. Sharma and R. N. P. Choudhary, *Mater. Lett*., 59 3921 (2005).
[61] A. Chen, Y. Zhi and L.E. Cross, *Phys. Rev*., B 62, 228 (2000).
[62] S. M. Blake, M. J. Falconer, M. McCreedy and P. Lightfoot, *J. Mater. Chem*., 7, 1609 (1997).
[63] S. Kojima, *J. Phys. : Condens. Matter*, 10, L327 (1998).
[64] Ismunandar and B. J. Kennedy, *J. Mater. Chem*., 9, 541 (1999).
[65] Y. Shimakawa, Y. Kudo, Y. Nakagawa, T. Kamiyama, H. Asano, and F. Izumi, *Phys. Rev*. B 61, 6559 (2000).
[66] Y. Noguchi, M. Miyayama, K. Oikawa and T. Kamiyama: Submitted *to Phys. Rev*.B.
[67] R. Macquart and B. J. Kennedy and Y. Shimakawa, *J. Solid State Chem*., 160, 174 (2001).
[68] I. Coondoo, A. K. Jha and S.K. Agarwal, (*Proceedings of the NSFD-XIII*) Nov 23 - 25 'o4, pp293.
[69] A. Chen, Y. Zhi, and J. Zhi, *Phys. Rev*., B 61, 957 (2000).
[70] A. Chen, J. F. Scott, Y. Zhi, H. Ledbetter, and J. L. Baptista, *Phys. Rev*. B59, 6661 (1999).
[71] L. E. Cross, *Ferroelectrics*, 76, 241 (1987).
[72] I. Coondoo and A. K. Jha, *Solid State Commu*., 142, 561 (2007).
[73] V. Shrivastava, A. K. Jha and R. G. Mendiratta, *Solid State Commu*., 133, 125 (2005).
[74] V. Shrivastava, A.K. Jha and R.G. Mendiratta, *Physica* B 371, 337 (2006).
[75] I. Coondoo, A. K. Jha, S.K. Agarwal and N. C. Soni, *J. Electroceram*., 16, 393(2006).
[76] Y. Noguchi, M. Miyayama, K. Oikawa, T. Kamiyama, M. Osada, and M. Kakihana, *Jpn. J. Appl. Phys*., 41, 7062 (2002).
[77] Y. Noguchi, A. Kitamura, L. Woo, M. Miyayama, K. Oikawa and T. Kamiyama, *J. Appl. Phys*. 94, 6749 (2003).
[78] T. Volk, L. Ivleva, P. Lykov, D. Isakov, V. Osiko and M. Wohlecke, *Appl. Phys. Lett*., 79, 854 (2001).
[79] T.-Y. Kim and H. M. Jang, *Appl. Phys. Lett*., 77, 3824 (2000).
[80] T. Watanabe, T. Kojima, T. Sakai, H. Funakubo, M. Osada, Y. Noguchi and M. Miyayama, *J. Appl. Phys*., 92, 1518 (2002).
[81] B. Frit and J. P. Mercurio, *J. Alloys and Compounds*, 188, 2694 (1992).
[82] B. H. Park, S. J. Hyun, S. D. Bu, T. W. Noh, J. Lee, H. D. Kim, T. H. Kim and W. Jo, *Appl. Phys. Lett*. 74, 1907 (1999).
[83] M. Villegas, A. C. Caballero, C. Moure, P. Duran and J. F. Fernandez, *J. Eur. Ceram. Soc*., 19, 1183 (1999).
[84] I. Pribosic, D. Makovec and M. Drofenik, *J. Eur. Ceram. Soc*., 21, 1327 (2001).
[85] T. Baiatu, R. Waser and K. H. Hardtl, *J. Am. Ceram. Soc*., 73,1663 (1999).
[86] J. J. Dih and R. M. Fulrath, *J. Am. Ceram. Soc*., 61, 448 (1978).
[87] W. L. Warren, K. Vanheusdan, D. Dimos, G. E. Pike and B. A. Tuttle, *J. Am. Ceram. Soc*., 78, 536 (1995).
[88] Q. Tan and D. Viehland: *Philos. Mag*. B 80,1585 (2000).
[89] C. Voisard, D. Damnajovic and N. Setter, *J. Eur. Ceram. Soc*., 19, 1251 (1999).

[90] D. Makovec, I. Pribosic, Z. Samardzija and M. Drofenik, *J. Am. Ceram. Soc*., 84, 2702 (2001).
[91] H. S. Shulman, M. Testorf, D. Damjanovic and N. Setter, *J. Am. Ceram. Soc*., 79, 3124 (1996).
[92] R. Gerson and H. Jaffe, *J. Phys. Chem. Solids,* 24, 979 (1963).
[93] M. Takahashi, *Jpn. J. Appl. Phys*., 10, 643 (1971).
[94] B. H. Venkataraman and K. B. R. Varma, *J. Phys. Chem. Solids* 66 (10), 1640 (2005).
[95] C. D. Wagner, W. M. Riggs, L. E. Davis and F. J. Moulder, *Handbook of X-ray Photoelectron Spectroscopy*, Perkin Elmer Corp., Chapman & Hall, 1990.
[96] S. Shannigrahi and K. Yao, *Appl. Phys. Lett*. 86(9) 092901 (2005).
[97] M. Miyayama, T. Nagamoto and O. Omoto, *Thin Solid Films*, 300, 299 (1997).
[98] T. Friessnegg, S. Aggarwal, R. Ramesh, B. Nielsen, E. H. Poindexter and D. J. Keeble, *Appl. Phys. Lett*., 77, 127 (2000).
[99] Q. Tan, J. Li and D. Viehland, *Appl. Phys. Lett*., 75, 418 (1999).
[100] I. K. Yoo and S. B. Desu, *Mater. Sci. Engg*., B13, 319 (1992).
[101] T. Watanabe, H. Funakubo, M. Osada, Y. Noguchi and M. Miyayama, *Appl. Phys. Lett*., 80, 100 (2002).
[102] Y. Noguchi, I. Miwa, Y. Goshima and M. Miyayama, *Jpn. J. Appl. Phys*., 39, L1259 (2000).
[103] S. Takahashi and M. Takahashi, *Jpn. J. Appl. Phys*., 11, 31 (1972).
[104] S. B. Desu, P. C. Joshi, X. Zhang and S. O. Ryu, *Appl. Phys. Lett*., 71, 1041 (1997).
[105] M. Nagata, D. P. Vijay, X. Zhang and S. B. Desu, *Phys. Stat. Sol*., (a)157, 75 (1996).
[106] J. J. Shyu and C. C. Lee, *J. Eur. Ceram. Soc*., 23, 1167 (2003).
[107] I. Coondoo, A. K. Jha and S.K. Agarwal, *Ferroelectrics*, 356, 31 (2007).
[108] T. Sakai, T. Watanabe, M. Osada, M. Kakihana, Y. Noguchi, M. Miyayama and H. Funakubo, *Jpn. J. Appl. Phys*., 42, 2850 (2003).
[109] C. H. Lu and C. Y. Wen, *Mater. Lett*., 38, 278 (1999).
[110] A. Li, D. Wu, H. Ling, T. Yu, M. Wang, X. Yin, Z. Liu and N. Ming, *Thin Sol. Films*, 375, 215 (2000).
[111] I. Coondoo, S.K. Agarwal and A. K. Jha, *Mater. Res. Bull*., 44, 1288 (2009).
[112] H. D. Sharma, A. Govindan, T. C. Goel and P. K. C. Pillai, *J. Mater. Sci. Lett*., 15, 1424 (1996).
[113] H. B. Park, C.Y. Park, Y. S. Hong, K. Kim and S. J. Kim, *J. Am. Ceram. Soc*., 82, 94 (1999).
[114] A. Garg and T. C. Goel, *J. Mater. Sci*., 11, 225 (2000).
[115] T. J. Boyle, P. G. Clem, B. A. Tuttle, G. L. Brennecka, J. T. Dawley, M. A. Rodriguez, T. D. Dunbar andW. F. Hammetter, *J. Mater. Res*., 17, 871 (2002).
[116] T. Takenaka and K. Sakata, *Ferroelectrics*, 38, 769 (1981).
[117] D. Wu, A. Li, T. Zhu, Z. Liu and N. Ming, *J. Appl. Phys*., 88, 5941 (2000).
[118] U. Chon, K. B. Kim and H. M. Jang, *Appl. Phys. Lett*., 79, 2450 (2001).
[119] J. Zhu, W. P. Lu, X. Y. Mao, R. Hui and X. B. Chen, *Jpn. J. Appl. Phys*., 42, 5165 (2003).
[120] S. L. Swartz, *IEEE Trans. Electr. Insul*., 25, 935 (1990).
[121] T. Ogawa and Y. Numamoto, *Jpn. J. Appl. Phys*., 41, 7108 (2002).
[122] A. Ando, T. Sawada, H. Ogawa, M. Kimura, and Y. Sakabe, *Jpn. J. Appl. Phys*., 41, 7057 (2002).
[123] I. S. Yi and M. Miyayama, *Jpn. J. Appl. Phys*., 36, L1321 (1997).

[124] C. Moure, L. Lascano, J. Tartaj and P. Duran, *Ceram. Int.*, 29, 91 (2003).
[125] C. Fujioka, R. Aoyagi, H. Takeda, S. O. Kamura and T. Shiosaki, *J. Eur. Ceram. Soc.*, 25, 2723 (2005).
[126] R. Jain, V. Gupta, A. Mansingh and K. Sreenivas, *Mater. Sci. Engg.*, B112, 54 (2004).
[127] R. Jain, A. K. S. Chauhan, V. Gupta and K. Sreenivas, *J. Appl. Phys.*, 97, 124101 (2005).

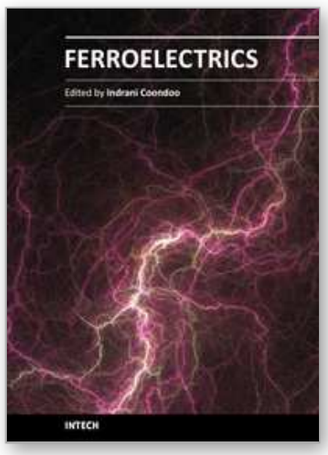

Ferroelectrics
Edited by Dr Indrani Coondoo

ISBN 978-953-307-439-9
Hard cover, 450 pages
Publisher InTech
Published online 14, December, 2010
Published in print edition December, 2010

Ferroelectric materials exhibit a wide spectrum of functional properties, including switchable polarization, piezoelectricity, high non-linear optical activity, pyroelectricity, and non-linear dielectric behaviour. These properties are crucial for application in electronic devices such as sensors, microactuators, infrared detectors, microwave phase filters and, non-volatile memories. This unique combination of properties of ferroelectric materials has attracted researchers and engineers for a long time. This book reviews a wide range of diverse topics related to the phenomenon of ferroelectricity (in the bulk as well as thin film form) and provides a forum for scientists, engineers, and students working in this field. The present book containing 24 chapters is a result of contributions of experts from international scientific community working in different aspects of ferroelectricity related to experimental and theoretical work aimed at the understanding of ferroelectricity and their utilization in devices. It provides an up-to-date insightful coverage to the recent advances in the synthesis, characterization, functional properties and potential device applications in specialized areas.

How to reference
In order to correctly reference this scholarly work, feel free to copy and paste the following:

Indrani Coondoo and Neeraj Panwar (2010). Enhanced Dielectric and Ferroelectric Properties of Donor (W6+, Eu3+) Substituted SBT Ferroelectric Ceramics, Ferroelectrics, Dr Indrani Coondoo (Ed.), ISBN: 978-953-307-439-9, InTech, Available from: http://www.intechopen.com/books/ferroelectrics/enhanced-dielectric-and-ferroelectric-properties-of-donor-w6-eu3-substituted-sbt-ferroelectric-ceram

INTECH
open science | open minds

InTech Europe
University Campus STeP Ri
Slavka Krautzeka 83/A
51000 Rijeka, Croatia
Phone: +385 (51) 770 447
Fax: +385 (51) 686 166
www.intechopen.com

InTech China
Unit 405, Office Block, Hotel Equatorial Shanghai
No.65, Yan An Road (West), Shanghai, 200040, China
中国上海市延安西路65号上海国际贵都大饭店办公楼405单元
Phone: +86-21-62489820
Fax: +86-21-62489821

IntechOpen